Inverting for Near Shore Bathymetry from Surface Wave Properties

Lasith Adhikari[1], Charnelle Bland[2], Lopamudra Chakravarty[3], Wenbin Dong[4],
Olaniyi Samuel Iyiola[5] Gail Muldoon[6] Clint Seinen[7]

Mentors: Lea Jenkins[8], Ty Hesser[9], Matthew Farthing[10]

Abstract

Tracking coastal bathymetry is necessary for marine navigation, military activities, and assessment and prediciton of storm damage as beaches evolve. Past efforts have derived surface wave properties from in situ bathymetric measurements. However, in situ measurements are costly and laborious to collect. As a result, direct observations of bathymetry are sparse in time and space. On the other hand, remotely sensed observations of surface conditions are becoming easier to obtain. We seek methods to invert for bathymetry given surface conditions.

We utilize linearized wave theory to estimate bathymetry near Duck, NC given measurements of surface wave properties collected by the U.S. Army Corps of Engineers. We process measurements of wave height, wave number, and bathymetry for easy incorporation into and validation of models. We also create a forward model to estimate wave number and wave height given bathymetry information. Several inverse methods including nonlinear least squares, Markov Chain Monte Carlo, and Tikhonov regularization then employ the data and forward model to estimate bathymetry along a one-dimensional profile.

Our results demonstrate good estimates of depth, h, in the near shore region, within 500 m of the beach. All inverse methods are able to accurately reconstruct a sandbar located in this region which is an important feature for consideration of rip tides and coastal navigation. Accuracy of the methods drops off past ~ 550 m from shore due to the increased depth and subsequent lower sensitivity of wave number to depth. We suggest several avenues for possible expansion of this work in the future which may improve overall accuracy of depth estimates.

1 Introduction

Bathymetry is a measurement of submarine topography and can be used to understand shifts of the ocean floor and its depth. Knowledge of bathymetry is important for marine navigation, both civilian and military, as well as for monitoring and predicting the effects of storms on coastal environments. While direct measurement of bathymetry is possible, the process tends to be cost and time prohibitive. For example, amphibious vehicles are capable of spatially limited surveys of bathymetry in difficult surf-zone conditions but require significant resources to operate. As a result of these factors, surveys tend to be sparse in time.

Current research focuses on a method to estimate bathymetry using surface measurements collected via remote sensing platforms, i.e. airborne, satellite, or onshore platforms. While bathymetry data is currently sparse due to observational limitations, the physics of waves are reasonably well understood. In particular, a dispersion relationship can be used to relate water depth to surface properties such as wave length and wave period. It is therefore possible to estimate bathymetry given observations of these parameters. Light Detection And Ranging (LiDAR) has been used to determine wave heights and Argus land-mounted video has been analyzed photogrammetrically to determine wave frequency and wave number. Both of these sources

[1]Applied Mathematics, University of California, Merced
[2]Mathematics & Statistics, University of West Florida
[3]Mathematical Sciences, Kent State University
[4]Civil Engineering, City College of New York
[5]Mathematical Sciences, University of Wisconsin-Milwaukee
[6]Geosciences, University of Texas Austin
[7]Mathematics & Statistics, University of Victoria
[8]Clemson University
[9]U.S. Army Corps of Engineers
[10]U.S. Army Corps of Engineers

therefore provide valuable inputs for estimating coastal bathymetry in a more efficient manner than is currently available.

Wave and bathymetric data has been collected in Duck, NC by the U.S. Army Corps of Engineers Coastal and Hydraulics Laboratory, including in situ measurements of bathymetry and measurements of the water surface. These measurements provide a method for testing algorithms to invert for bathymetry because the true bathymetry is available for comparison to the numerical estimates.

In Section 2 we discuss...etc.

2 The Problem

Although there have been uncertainties in capturing the topography of the ocean near shore, mathematical methods can estimate bathymetry using the dispersion relationship between wavelength and the period. Stockdon et al. used video imagery, which compared true wave signal and remotely sensed video signal to create a linear representation between wave amplitudes and phases [3]. Holman et al. used a 2-dimensional method with Kalman filtering to estimate the depth, h [1].

We invert for depth, h, using wave length and wave number with a 1D model derived using the energy flux method to create a correlation between wave length and depth from the water surface as shown in Figure **??**.

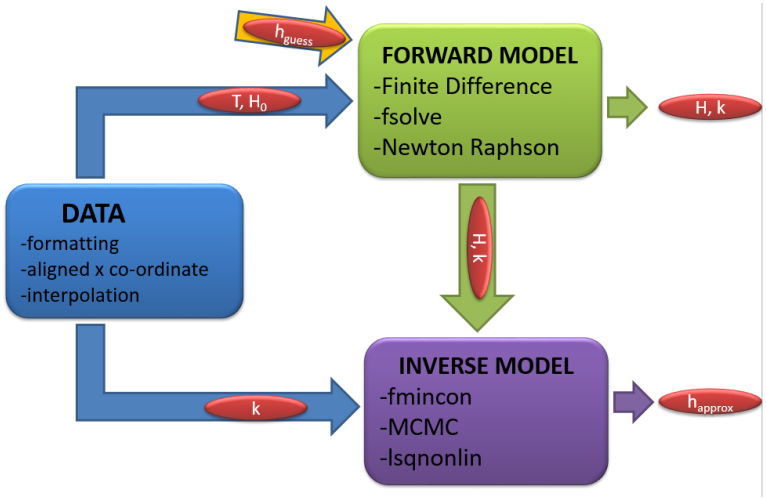

Figure 1: Flow chart of the workflow for this research

2.1 Forward Problem

The forward problem is described by 1D linear wave theory:

$$\frac{d}{dx}\left(EC_g\right) = -\delta, \tag{1}$$

$$\begin{cases} \frac{d}{dx}\left(EC_g\right) = -\delta, \\ \sigma^2 = gk\tanh(kh), \end{cases} \tag{2}$$

where δ is wave breaking parameter and the speed at which the energy is transmitted, C_g, called linear theory group speed, is given as

$$C_g = \frac{c}{2}\left(1 + \frac{2kh}{\sinh(2kh)}\right), \tag{3}$$

with $c = \frac{\sigma}{k}$ and from the linear theory, the wave energy, E is given as

$$E = \frac{1}{8}\rho g H^2, \tag{4}$$

ρ is the density of water, g is the gravitational acceleration, σ is the angular frequency, c is the local wave phase speed, k is the wave number, h is the water depth and H is the wave height. Here, we assume T, the wave period, is constant.

Observe that equation 2 is coupled using the fact that $\sigma = \frac{2\pi}{T}$. Hence, using equation 3 and 4 in 2, we obtain

$$\frac{d}{dx}\left(\frac{\lambda}{k}\left(1 + \frac{2kh}{\sinh(2kh)}\right)H^2\right) = -\delta, \tag{5}$$

and

$$f(k) = gk\tanh(kh) - \sigma^2, \tag{6}$$

where k is the zero of function f and $\lambda = \frac{\rho g \pi}{8T}$.

The wave breaking function, δ, proposed by (Janssen and Battjes, 2007) is given as

$$\delta = \frac{1}{4h}B\rho g f H_{rms}^3\left[(R^3 + \frac{3}{2}R)exp(-R^2) + \frac{3}{4}\sqrt{\pi}(1 - erf(R))\right], \tag{7}$$

This breaking function is basically depends on the wave height H using the following parameters in terms of H

$$R = \frac{H_b}{H_{rms}}, \quad H_{rms} = 0.7H, \quad H_b = 0.78h, \quad f = \frac{1}{T}, \quad B = 1.$$

In the above expression H_b is the local wave breaking height influenced by the breaking condition in the shallow water. H_{rms} gives the root mean square of height. and f represents frequency. We can see that R is wave breaking condition is provided

2.2 Numerical Solution of the Forward Model

An upwinding scheme is applied to obtain a numerical solution with appropriate initial and boundary conditions.The goal is to provide wave height from the model equation (1). In the process, MATLAB's fsolve function is applied to obtain the wave number. Furthermore, the Newton-Raphson method is used to verify the solution of wave number k obtained by the fsolve function.

2.2.1 Discretization and Implementation of the Model

To apply the upwinding method we first discretize the space vector, x, depending on predefined mesh size, Δx. For the numerical experiments we applied $\Delta x = 10$ and $\Delta x = 25$ which means index points are set in $10m$ and $25m$ apart respectively.We have applied equal spacing for this numerical scheme. Depending on the Δx the wave height$H$ will be computed at each index point from the model equation . In the process we calculate the following terms:
Total energy per unit area

$$E = \frac{1}{8}\rho g H_{rms}^2$$

where ρ is water density $1000kg/m^3$ and g represents the gravitational acceleration $9.8m/sec^2$.
The root mean square of height as

$$H_{rms} = 0.7H$$

Group wave celerity will be defined as in (3). The wave period is provided from the original data with boundary

condition H_0. Wave number plays an important role in estimating the wave height as well. Wave number is employed through the group celerity C_g.To calculate the wave number MATLAB function fsolve used as non-linear solver to find the zeros of the function given in (6). So, at each index point, wave number, k, is generated with initial guess k_0:

$$k_0 = \frac{\sigma}{\sqrt{gh}}.$$

This initial condition is chosen, because in shallow water the dispersion relation provides

$$\sigma^2 \simeq g\,k^2\,h$$

Newton-Raphson method is applied to verify the wave number from fsolve. Therefore, using same initial condition the approximate solution is obtained from

$$k_{i+1} \quad = \quad k_i - \frac{gk_i \tanh(k_i h) - \sigma^2}{g\tanh(k_i h) - ghk_i sech^2(k_i h)}, \tag{8}$$

Wave breaking condition is passed via the breaking function δ at each step of the computation. Thus at each index forward finite difference expression is calculated as

$$E_i = \frac{\delta_{i-1}\Delta x}{(C_g)_i} + \frac{E_{i-1}(C_g)_{i-1}}{(C_g)_i}$$

After estimating the energy E at each index points we update the value of the root mean square of height H_{rms}. This updated value is applied in the $H = \frac{H_{rms}}{0.7}$ to obtain the wave height at each index points.

The implementation of the algorithm is as follows

Algorithm 1 Algorithm to estimate wave height H

procedure
Initialization:
Mesh spacing: Δx
Initial depth: h
Wave period: T
Boundray condition of height: H_0
Step 1: Estimate wave number k
- $\sigma = \frac{2\,\pi}{T}$
- $\sigma^2 = gk\tanh(kh)$

Step 3:Compute wave height H
for $i = 1, 2, ..., N$
- *Compute wave breaking function:* δ
- *Compute wave group celerity:* C_g
- *Compute:* $E_i = \frac{\delta i-1 * \Delta x}{(C_g)_i} + \frac{E_{i-1} * (C_g)_{i-1}}{(C_g)_i}$
- *Update :* $(H_{rms})_i = \sqrt{\frac{8.0\,E_i}{\rho\,g}}$
- *Compute :* $H_i = \frac{(H_{rms})_i}{0.707}$

2.2.2 Numerical Results

We present some of the numerical results in the following Figures.

Figure 2 shows that the wave height is positively correlated to the depth. We can see the similar characteristics between depth and wave number. This is the reason for why we can perform the simulation by providing H or k to obtain the depth h. The wave height curve and wave number curve will rapidly increase to a significant level around where depth is very close to zero, and the data there is not reliable because of the poor behavior of equations around $h = 0m$ (We need to force wave height to zero when depth is close to zero, or the wave height given by those equations will turn to infinity). However, the shape of wave height curve or

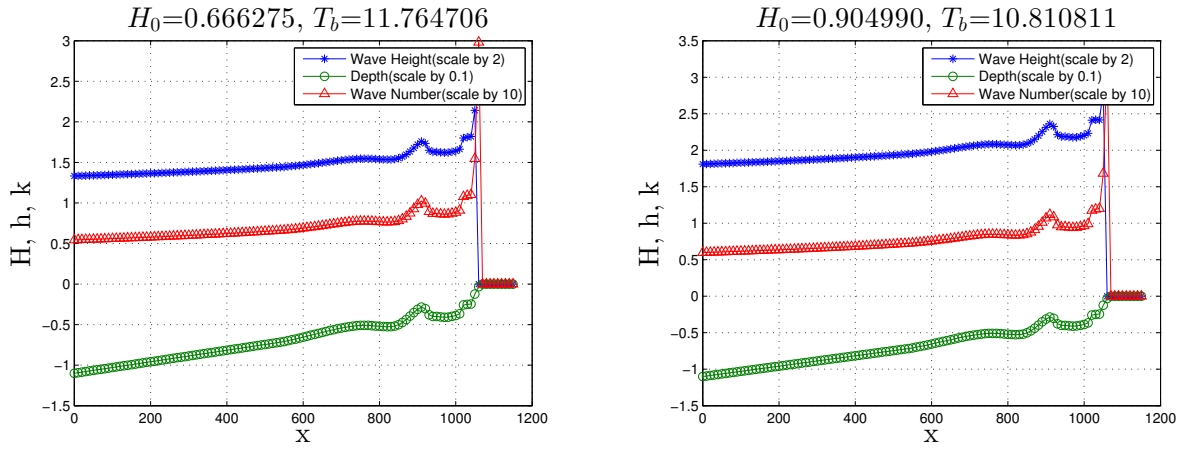

Figure 2: Water Depth(h), Wave Height(H) and Wave Number vary along x direction (Two sets of boundary conditions are applied for following figures. The boundary conditions for the left is extracted from the data of 2015/10/9 22:00-23:00 and for the right is extracted from the data of 2015/10/9 03:00-04:00). Note that $x = 0m$ is located offshore at the boundary point.

wave number curve around the peak of depth curve shows our model has a reasonable good response to the changing depth.

Figure 3 shows the shallow water assumption which is $h * k << 1$ (The red horizontal line is $h * k = 1$). We can see that our model is well fit the criteria at most data points except some where their depths are close to zero.

Figure 4 is the variation of wave energy along x-axis. The energy will accumulate unless the wave height meets the break condition.

Figure 5 is the variation of wave phase speed (celerity) along x-axis. As celerity is a function of wave number and wave period (wave period is assumed to be fixed in our case).

Figure 6 shows the variation of wave height along with depth. The data at zeros should not be taken into consideration.

Figure 7 shows the variation of wave energy along with wave height. The data at zeros should not be taken into consideration. As the energy is calculated by $E = \frac{1}{8}\rho g H^2$, the curve is a part of $y = x^2$.

Figure 8 is the variation of wave energy dissipation along x-axis. Just as the basic assumption of our model, the energy does not dissipate significantly until the depth becomes relatively small (the after the main peak is not reliable as the depth there is too small). The small peak around $x = 900m$ is caused by the peak part of the bathymetry.

3 Data

Data for this project were collected by the U.S. Army Corps of Engineers (USACE) Engineer Research and Development Center (ERDC) during October 2015 at the Field Research Facility (FRF) in Duck, NC on the Outerbanks shown in Figure 9.[11] The data was collected via the BathyDuck project conducted by the Coastal and Hydraulic Laboratory (CHL). Data of interest includes wave height (H), wave number (k), wave period (T), and bathymetry (h) measurements. These data combine information collected through a Nortek Acoustic Wave and Current (AWAC) Profiler, a Light Amphibious Resupply Cargo (LARC-5) vessel, a Coastal Research Amphibious Buggy (CRAB), and Argus Beach Monitoring systems. The LARC-5 and CRAB vessels are shown below in Figure 10.

The following sections discuss in more detail the observations and how they were used. Note in physical space, the boundary point used for the 1-dimensional problem is located 1150 m offshore. For numerical

[11] The data is available in netcdf format at http://chlthredds.erdc.dren.mil/thredds/catalog/frf/projects/bathyduck/catalog.html

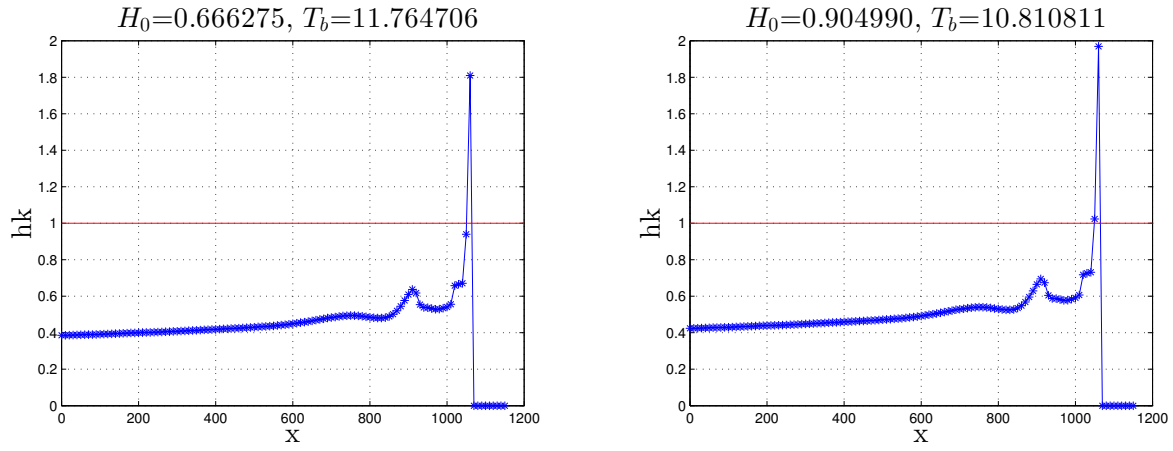

Figure 3: Relative Depth varies with x direction

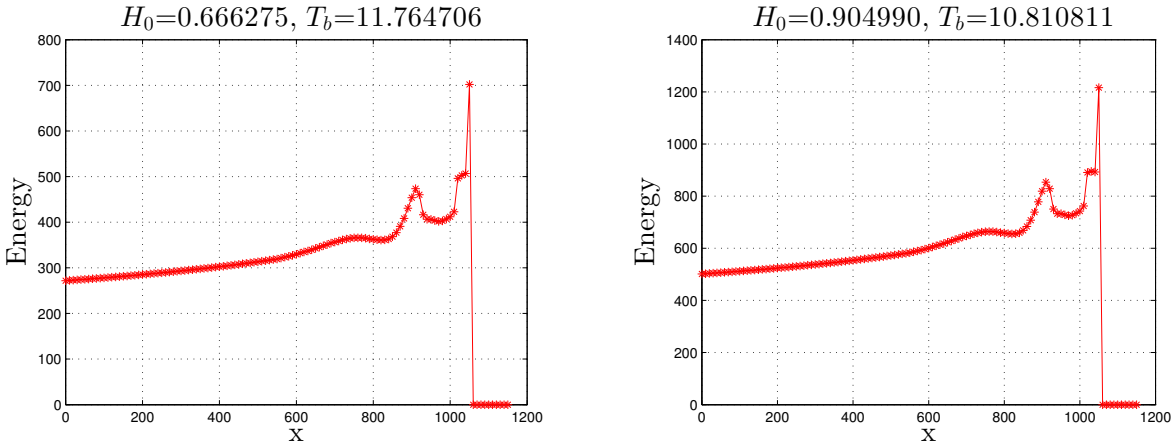

Figure 4: Wave Energy varies with x direction

simplicity, all observations are transformed such that $x = 0$ m corresponds to the offshore boundary point and $x = 1150$ m is the shoreline.

3.1 Boundary Condition

Boundary conditions for this project were collected through a bottom-mounted AWAC profiler located approximately 1150 meters offshore at a depth of 11 meters (Figure 11).

Vast amounts of wave data has been collected by the AWAC system at the offshore boundary. For the 1-dimensional problem, the forcing condition at this boundary is the significant wave height and peak frequency.

3.2 Bathymetry

Survey data collected on 1 October 2015 was considered for this analysis. These data were measured via the CRAB and Trimble Real Time Kinematic (RTK) GPS system. Elevation data from six cross-sections[12], perpendicular to the shoreline, spaced over a 100-meter portion of the beach were combined to create the 2D surface shown in Figure 12.

[12] we could potentially add an overhead plot of the transects

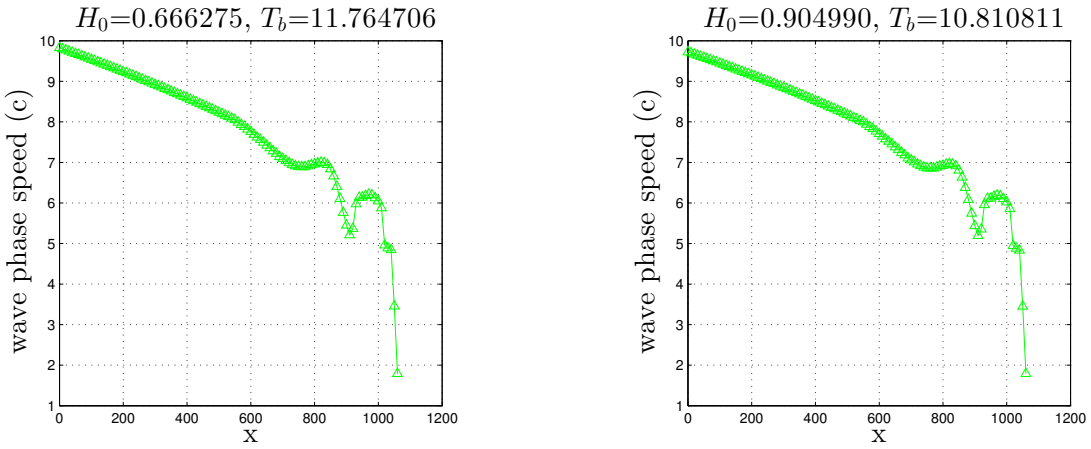

Figure 5: Wave Phase Speed (c) varies with x direction

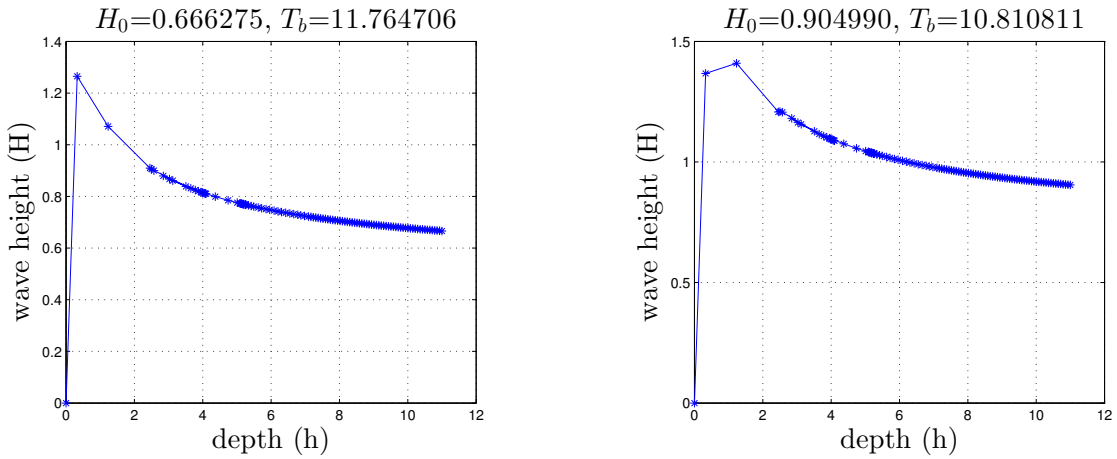

Figure 6: Wave Height(H) varies with Water Depth(h)

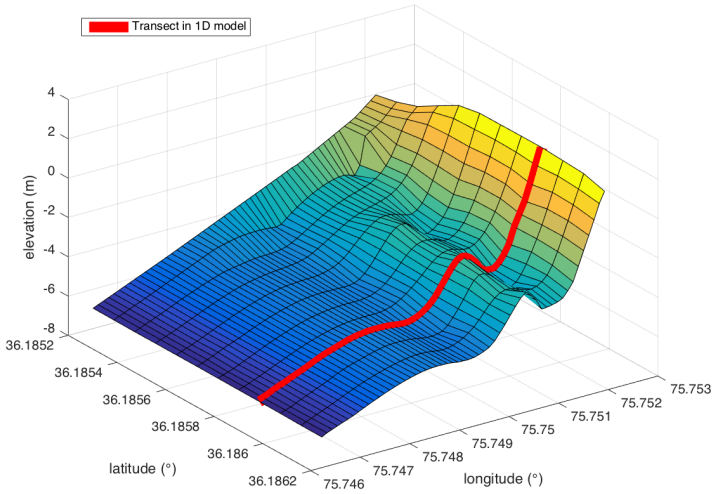

Figure 12: Measured and gridded 2D bathymetry in the survey area on 1 October 2015. The red line shows the transect considered in the 1D problem.

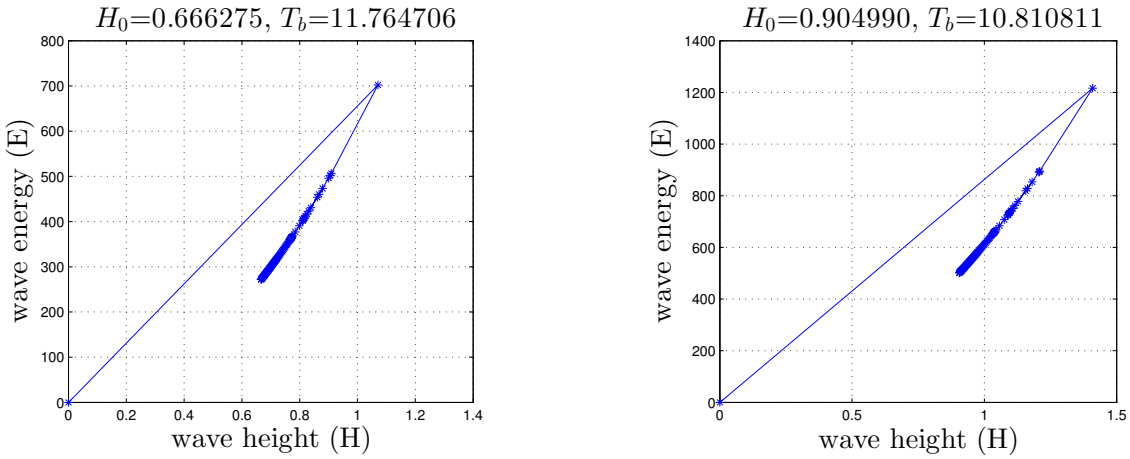

Figure 7: Wave Energy varies with Wave Height(H)

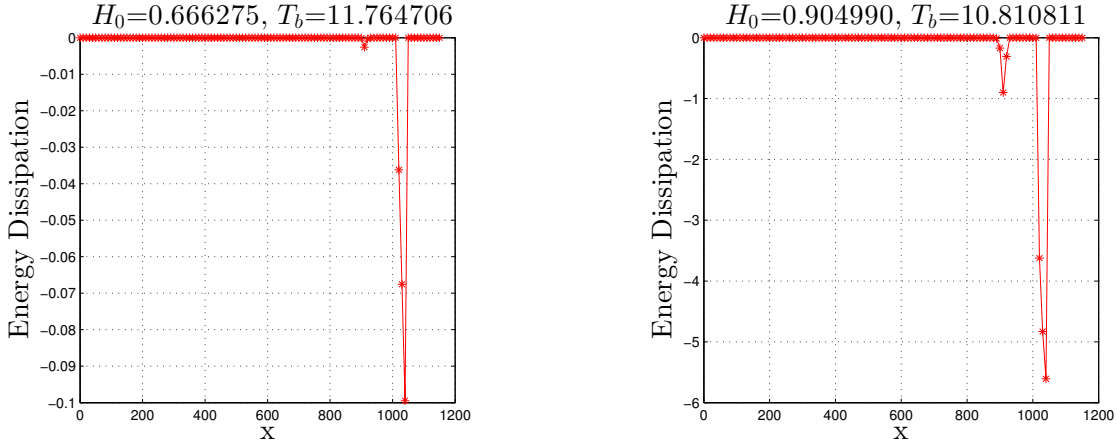

Figure 8: Wave Energy Dissipation varies along x-axis

For the 1D problem, a single slice of the 2D bathymetry was used as model input, identified by the red line in Figure 12. In a cartesian coordinate system, this line (a.k.a. 'transect') is located at $y = 950$ meters.

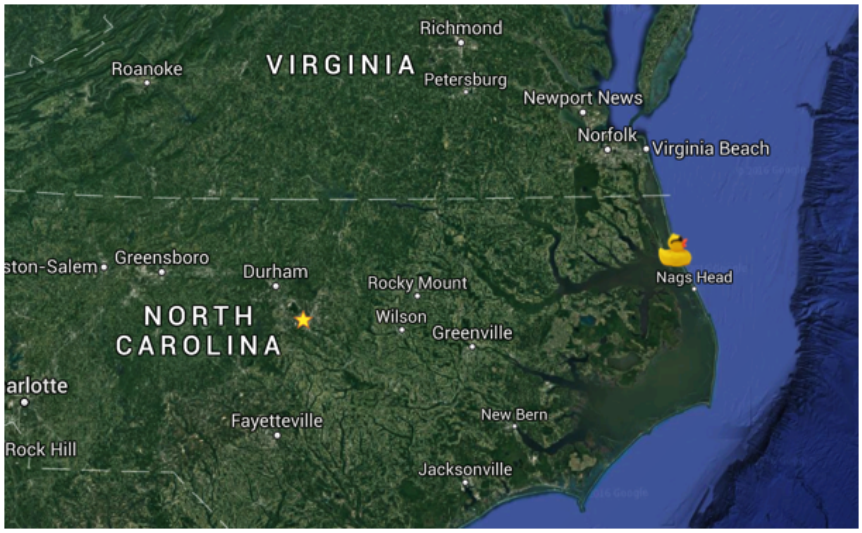

Figure 9: The location of the U.S. Army Corps of Engineers Field Research Facility in Duck, NC.

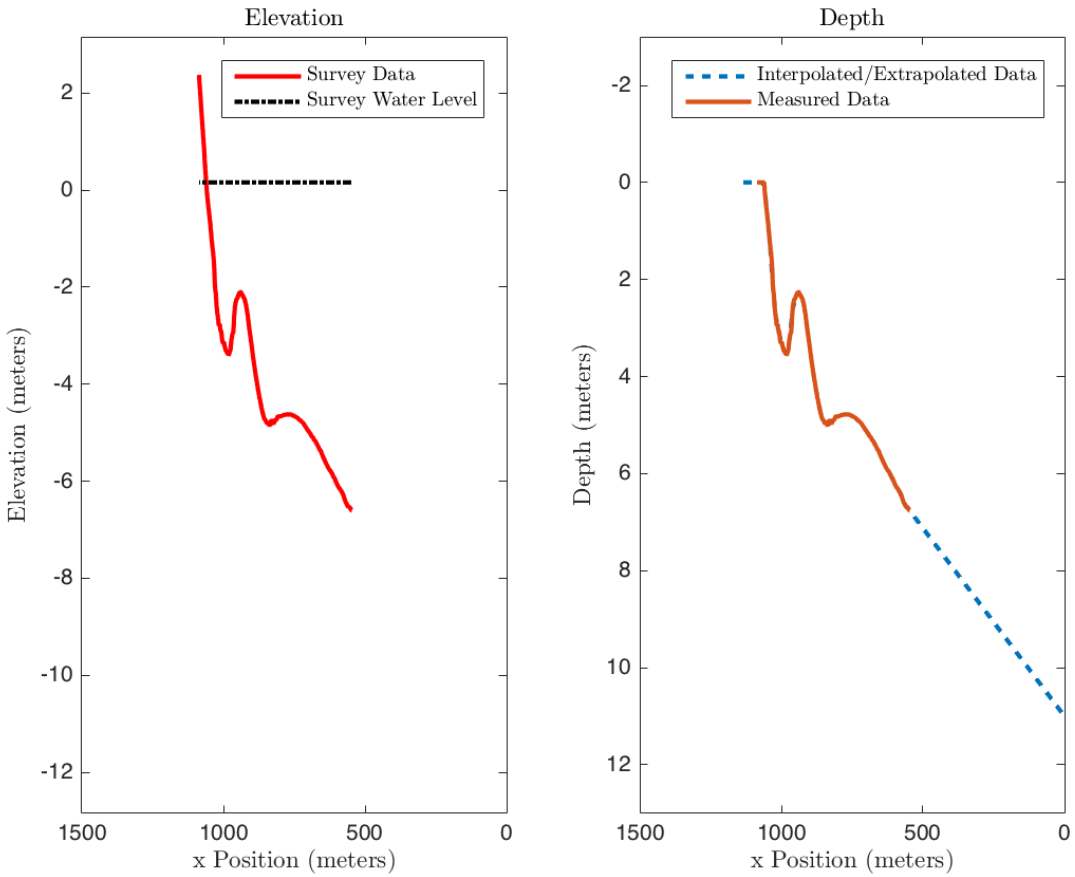

Figure 13: 1D Bathymetry - elevation data (left) and depth data (right).

Figure 10: The LARC (left) and CRAB (right) instruments are used to measure near coastal bathymetry. Image source: http://www.frf.usace.army.mil/aboutUS/equipment.shtml

Survey data provided sea floor elevation referenced to the North American Vertical Datum of 1988 (NAVD88) (Figure 13, *left*). To provide proper input data for the 1D model, elevation was transformed to depth data (Figure 13, *right*). Once transformed, depth was discretized by interpolating between measured data points via Matlab's built-in pchip method. Pchip was chosen for the interpolation due to its shape-preserving nature so as to not introduce non-physical oscillations. Between the boundary condition and the nearest measured depth point, linear interpolation was used to fill in missing data.

3.3 Wave number

Wave number is a measure of the number of waves per unit distance and is inversely proportional to wave speed. Hourly observations using an Argus video monitoring system mounted on shore are available during October 2015. Photogrammetry is performed on the video to derive the dominant wave frequencies and wave numbers in the survey area [1]. Data is available for a 2D area at the FRF survey site. A 1D profile is extracted from the 2D data along a transect corresponding to the position of the model boundary point ($y = 950$ m). Figure 14 shows statistics for wave number, k, along the 1D transect. Wave number is shown to be slightly more variable over time close to the coast. Mean wave number increases toward the shoreline, as expected.

Figure 11: Acoustic Wave and Current Profiler. Image source: http://www.nortek-as.com/en/products/wave-systems/awac

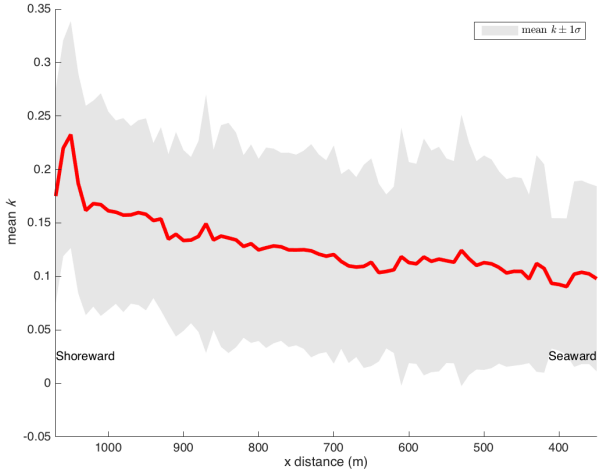

Figure 14: Wave number along the transect where the model boundary condition is located. Mean wave number, k, during October 2015 is shown in red. Gray envelopes show $\pm$ 1σ standard deviation in k. Wave number is observed to be relatively larger and more variable closer to shore.

4 Inversion Methods

[Introduction please...]

4.1 The Additive Gaussian Noise Model

By assuming the measurements are corrupted by the additive Gaussian noise, the linear estimation model can be written as

$$\mathbf{d} \sim \text{Gaussian}(\mathbf{A}\mathbf{h}_t), \tag{9}$$

where

$\mathbf{d}$ = a vector of measurements,
$\mathbf{A}$ = a linear forward operator,
$\mathbf{h}_t$ = the true bathymetry (depth).

Therefore, a Gaussian noise $\boldsymbol{\epsilon}$ corrupted measurements $\mathbf{d}$ with a standard deviation ν is given by

$$\mathbf{d} = \mathbf{A}\mathbf{h}_t + \boldsymbol{\epsilon}.$$

4.2 Ordinary Least-Squares Inversion

As a beginning to approximate the topographic heights of the near-shore sea-floor, we consider the following least-squares minimization problem,

$$\hat{\mathbf{h}} = \underset{\mathbf{h}\in\mathbb{R}^n}{\arg\min} \quad f(\mathbf{h}) = \|\mathbf{A}\mathbf{h} - \mathbf{d}\|_2^2, \tag{10}$$

where we minimize the data misfit between the forward predictions and the measurements, in the least-squares sense. In order to test possible Matlab inbuilt solvers to solve the minimization problem in (10), we have generated dummy measurements with $\nu = 0.1$. In particular, in this test, the forward operator `A = rand(50)`, the true bathymetry `ht = -linspace(-11,0,N)' - 11`, and the Gaussian noise corrupted measurements `b = A * h_t + 0.1 * randn(N,1)`. Recovered bathymetries from different Matlab solvers are given below. Note that the initial guess for all methods is zero.

(1) *Nonnegative least-squares method:* `lsqnonneg(A,b, options)`. This Matlab function uses the algorithm so called *active-set* and note that it requires the matrix $\mathbf{A}$ explicitly. Residual norm error for this nonnegativity reconstruction is 8.88×10^{-26} (see Fig. 15).

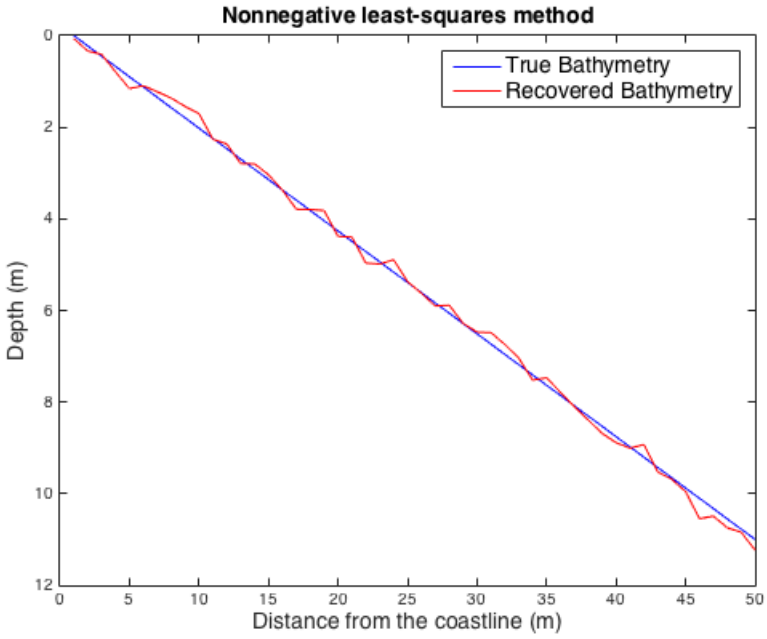

Figure 15: Nonnegative least-squares method reconstruction of depth $\mathbf{h}$ using the dummy dataset.

(2) *Trust-Region-Reflective method:* `lsqnonlin(@(h) A * h - b, zeros(N,1), zeros(N,1),inf(N,1), options)`. Note that the reconstruction of $\mathbf{h}$ is restricted to the positive x-axis using the function arguments. Residual norm error for the reconstruction is 4.32×10^{-10}.

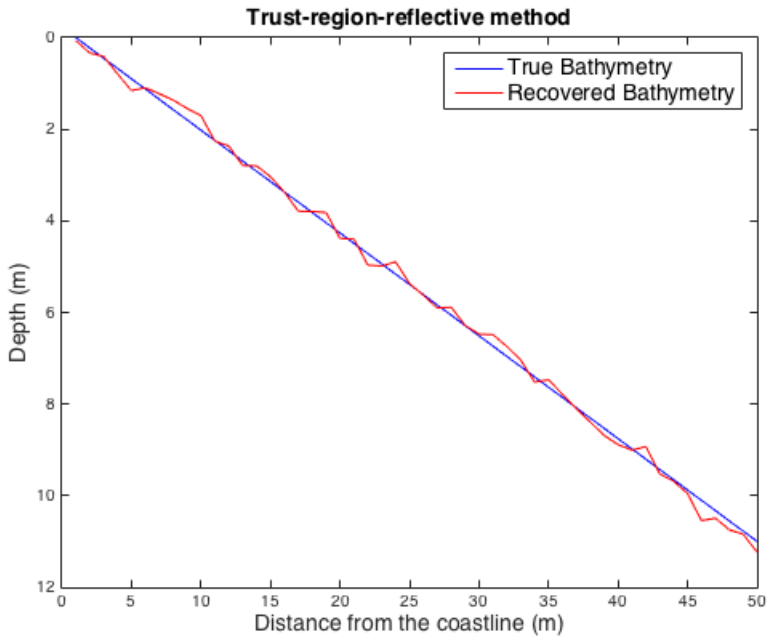

Figure 16: Trust-Region-Reflective method reconstruction of depth **h** using the dummy data.

(3) *Levenberg-Marquardt (LM) method:* `lsqnonlin(@(h) A * h - b, 'Algorithm', 'levenberg-marquardt')` Residual norm error for the reconstruction is 6.39×10^{-13}. The Levenberg-Marquardt algorithm does not handle bound constraints.

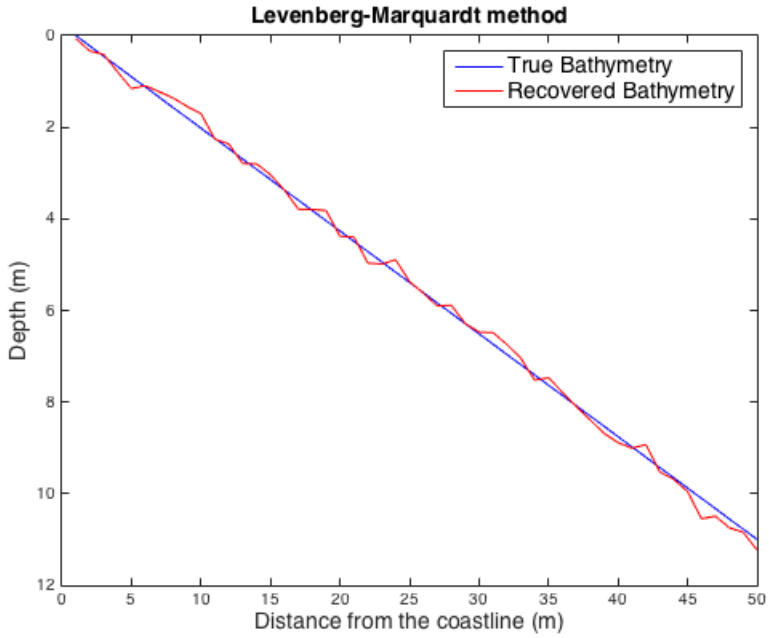

Figure 17: Levenberg-Marquardt (LM) method reconstruction of depth **h** using the dummy data.

(4) *Interior-point method:* `fmincon(f, zeros(N,1), [],[],[],[], zeros(N,1), inf(N,1))`. Residual norm error for the sample dummy data set with $\nu = 0.1$ is 1.29.

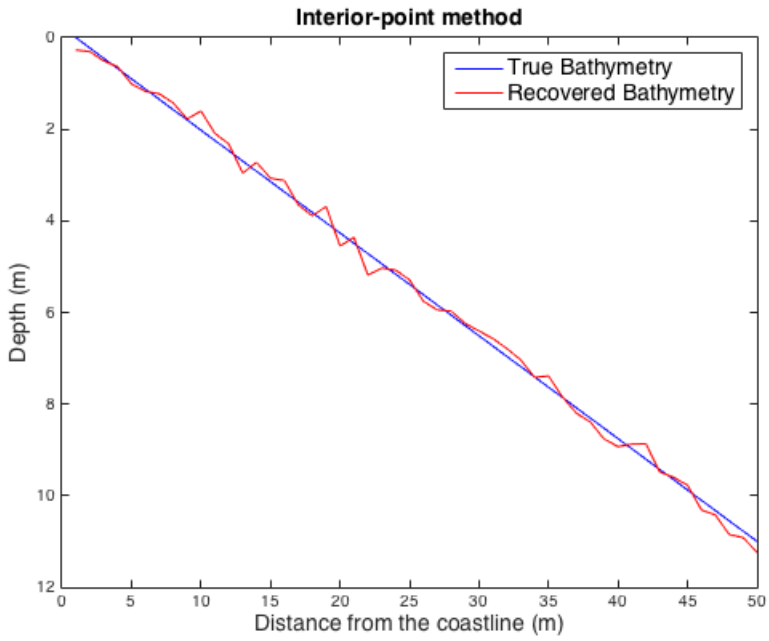

Figure 18: fmincon method reconstruction of depth $\mathbf{h}$ using the dummy data.

4.3 Tikhonov Regularization

Although the ordinary least squares solution can deal with well-posed problems (i.e. the solution exist and unique), it might yield into a unstable solutions in the presence of a small noise in the measurements. Due to the ill-conditioned nature of the forward operator matrix $\mathbf{A}$, the noise components of the observations can be amplified and leads into a drastic change in the solution. To overcome this problem, we use *regularization*. The Tikhonov regularization is one of the most widely used regularization techniques in the inverse problems community. It couples the least squares term in (10) with a additional regularization term as defined by

$$\hat{\mathbf{h}} = \underset{\mathbf{h}\in\mathbb{R}^n}{\arg\min} \ \ \|\mathbf{A}\mathbf{h} - \mathbf{d}\|_2^2 + \alpha\|\mathbf{h}\|_2^2 \tag{11}$$

where α is the regularization parameter (> 0), which balances the trade-off between data fidelity term (i.e, the least squares term) and the regularization term $\|\mathbf{h}\|_2^2$. Last but not least, the ordinary least squares method can not incorporate any prior knowledge about the bathymetry, for e.g., any known depths near the shore. However, If we have some prior depth estimate $\mathbf{h}_p$ for the $\mathbf{h}_t$, then the Tikhonov regularized solution with the prior information can be written as

$$\hat{\mathbf{h}} = \underset{\mathbf{h}\in\mathbb{R}^n}{\arg\min} \ \|\mathbf{A}\mathbf{h} - \mathbf{d}\|_2^2 + \alpha\|\mathbf{h} - \mathbf{h}_p\|_2^2, \tag{12}$$

where α is a regularization parameter (> 0). To test this method in (12), Tikhonov method is implemented and test with sample data set with $\nu = 0.2$. This reconstruction of depth has 0.038 residual norm error. In order to run this `tikhonov` Matlab function, matrix $\mathbf{A}$ should be explicitly known.

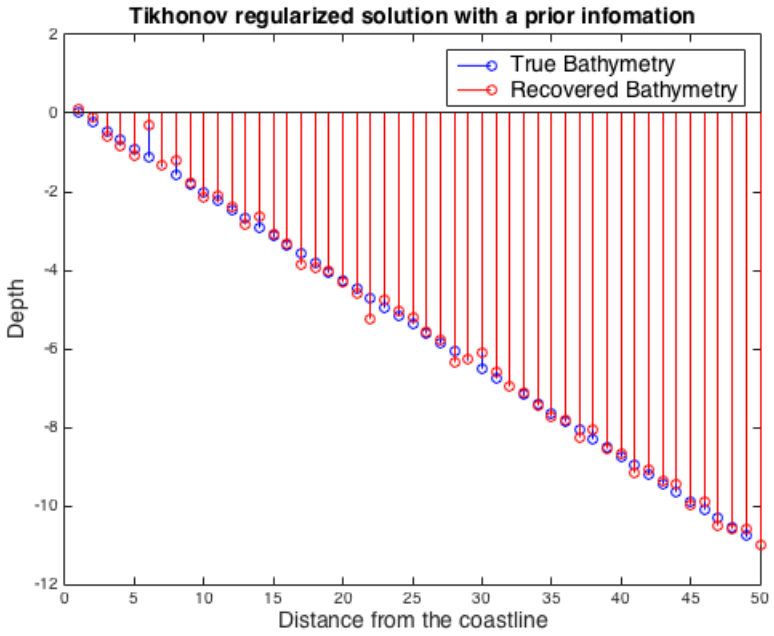

4.4 Bayesian MCMC Inverse Method

We implement a Bayesian approach because this method uses past information about the parameter, h, to form a prior distribution for analysis and it will sample the posterior probability distribution of "true" h. The recovered distribution of h profiles allows for an intuitive understanding of uncertainty in estimated h.

4.4.1 Bayesian Formulation

We use a Bayesian Markov Chain Monte Carlo (MCMC) method to estimate depth, h, given wave number, k. This method computes the posterior probability distribution of h by combining prior information about h with a likelihood function according to Bayes Rule in Equation 13:

$$P(h|k) \propto \Pi(h)L(h|k), \tag{13}$$

where $P(h|k)$ represents the posterior probability function, $\Pi(h)$ is the prior distribution function and $L(h|k)$ is the likelihood function.

We create a random walk Metropolis algorithm [2] which samples proposed depth profiles and updates the posterior probability distribution of h according to the likelihood that the proposed depth profiles describe the true bathymetry.

To estimate depth, we create a prior distribution function of h given 500 realistic approximations of bathymetry derived by the U.S. Army Corps of Engineers. We assume a normal conjugate prior with mean and standard deviation determined by the distribution of simulated bathymetry as shown in equation 14, this ensures our posterior distribution is normal as well.

$$\Pi(h) \sim N(0, \sigma^2_{sim}) \tag{14}$$

where $\sigma^2_{sim} = 1.01\ m$ is the variance of the simulated h profiles.

Given the sample bathymetry, we evaluate the forward model to compute wave numbers along the 1D profile. A likelihood function (Equation 15) compares the computed k profile to k values observed along the 1D profile.

$$L\left(h|k\right) = \exp\left(-\frac{\sum_{i=1}^{n}(k_{m,i} - k_{d,i})^2}{2\sigma_d^2}\right) \tag{15}$$

Modeled and observed k are $k_{m,i}$ and $k_{d,i}$, respectively, where i corresponds to the points along the 1D profile for which we have inferred k measurements and σ_d^2 is the variance of k values observed along the 1D profile during October 2015. (See section 3.3 for more information about the observations.)

The likelihood uses the sum of square errors between simulated and observed k to quantify the probability that the modeled k represents the true k profile as observed. Inclusion of the σ_d^2 acknowledges that a perfect match between modeled and observed k cannot be expected due to uncertainty in the measurements of k.

4.4.2 Metropolis Algorithm

The Metropolis algorithm begins with an initial h profile sampled from the simulated distribution of bathymetry. This initial estimate of h is used to compute an initial prior probability distribution. An initial likelihood probability distribution is computed using observed values of k, modeled values of k determined by using the sampled h as input to the forward model (see Section 2.1), and σ_d^2. The prior and likelihood are combined to compute an initial posterior probability distribution of h, shown in equation 16:

$$P(h|k) = log[\Pi(h)] + log[L(h|k)] \tag{16}$$

The algorithm then uses a markov chain random walk to propose new h profiles. Each proposed h is evaluated in the forward model to get a proposed k profile. The proposed k is then compared to observed k using the likelihood function and a proposed posterior distribution is computed.

A unique characteristic of the Metropolis algorithm is the way in which proposed posteriors are accepted or rejected by comparison to the previous step's posterior probability. The probabilty of accepting a proposed posterior is

$$\rho = exp[P(h|k)_{prop} - P(h|k)_{current}] \tag{17}$$

The formulation in equation 17 implies that if the proposed posterior probability is higher than the current posterior probability then the proposed posterior probability replaces the current posterior probability and the proposed h is accepted as a solution. The algorithm is then incremented and a new proposal is selected and evaluated.

4.4.3 Verification

The Metropolis algorithm used for this project was developed by the authors. To verify the algorithm is working correctly, it was tested on a simple ODE:

$$y = \alpha x \tag{18}$$

where the goal is to estimate the value of α.

5 Estimating Bathymetry

In this Section, we describe some experimental results with simulated and real data using few existing nonlinear optimization tools that we used in our preliminarily experiments (see Section 4). Note that our forward model is nonlinear as described in Section 2.1 and it can not be written as a matrix equation system. Therefore, in this Bathymetry inversion, we can not use any inverting method where it needs forward operator as a explicit matrix operator (e.g., `tikhonov` and `lsqnonneg` Matlab® functions need forward operator as a matrix). Moreover, the bounds of the true Bathymetry range in the interested near shore region is known to be $[0m, 11m]$. Therefore, we picked the inverse solvers that enables us to incorporate that prior knowledge too.

5.1 Simulated Data

In this study, Gaussian noise corrupted simulated wave numbers (see Section 4.1 for more details) are generated by

$$\mathbf{k}_s = A(\mathbf{h}_t) + \mathcal{N}(0, \nu^2), \tag{19}$$

where $A(\cdot)$ represents the nonlinear forward operator defined in Section 2.1, $\mathbf{h}_t \in \mathbb{R}^n_+$ is the true Bathymetry vector, and $\mathcal{N}(0, \nu^2)$ is a additive Gaussian noise vector with standard deviation ν, generated in the Matlab® by $\nu \cdot$ `randn(n,1)`. we manufactured wave numbers $\mathbf{k}_s$ for two different grid resolutions, i.e., 10m and 25m (see Fig. 20 and 19 respectively), to test and tune our inverse methods before working with actual measurements.

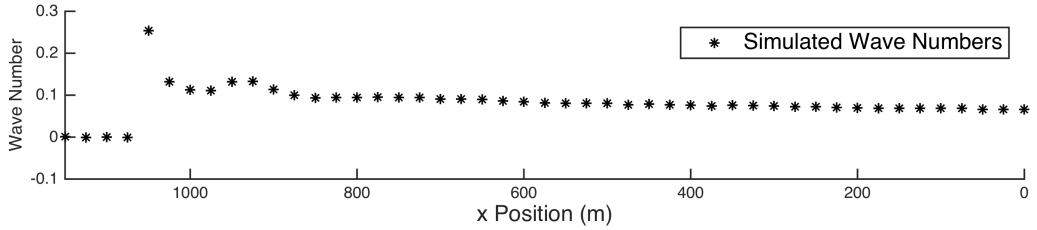

Figure 19: 1% noisy ($\nu = 10^{-3}$) simulated wave numbers (k) with 25m grid resolution. Noise (%) $= \|A(\mathbf{h}_t) - \mathbf{k}_s\|/\|\mathbf{k}_s\| \cdot 100$.

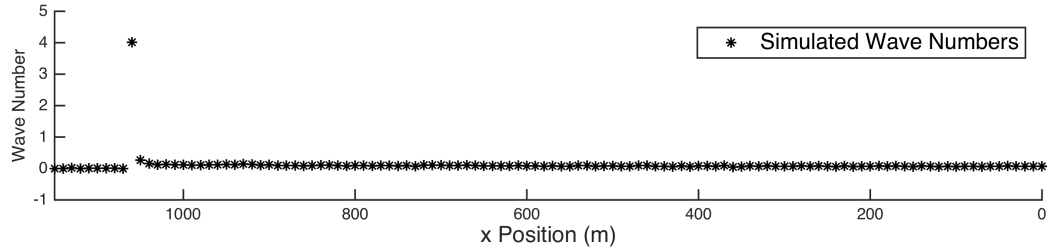

Figure 20: 2.5% ($\nu = 10^{-2}$) noisy simulated wave numbers (k) with 10m grid resolution. Noise (%) $= \|A(\mathbf{h}_t) - \mathbf{k}_s\|/\|\mathbf{k}_s\| \cdot 100$.

5.2 Real Data

Measured wave numbers (see Fig. 21) by US Army Corps of Engineers (USACE) at the field research facilities in Duck, NC on 09th October 2015 is used to approximate the true bathymetry using different inversion schemes. Note that the measured wave numbers near the shore (x Position $>$ 1050m) and the deep end (x Position $<$ 350m) are not available for our numerical experiments.

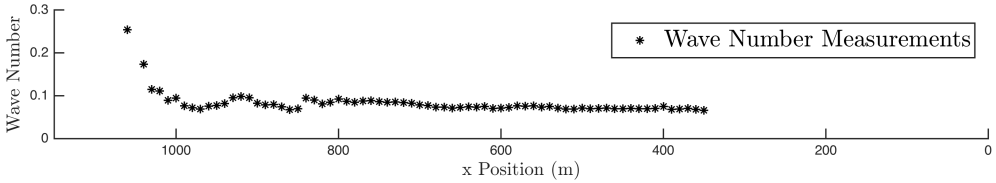

Figure 21: Real measurements of wave numbers (k) on the 09th October 2015 at 21:59 by the US. Army Corps of Engineers (USACE) Engineer Research and Development Center (ERDC).

5.3 Ordinary Least-Squares Fitting

$$\hat{\mathbf{h}} = \underset{\mathbf{0} \preceq \mathbf{h} \preceq \mathbf{11}}{\arg\min} \ \|\mathbf{A}(\mathbf{h}) - \mathbf{d}\|_2^2, \tag{20}$$

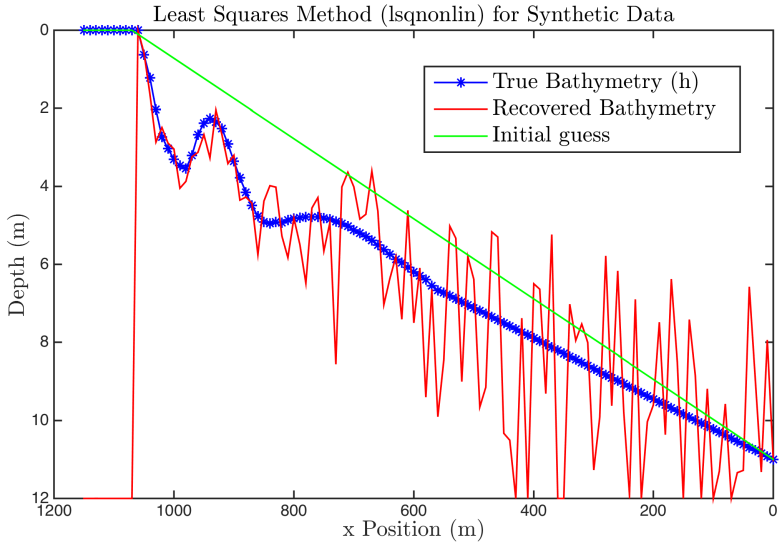

Figure 22: lsqnonlin method reconstruction of depth $\mathbf{h}$ using the simulated data.

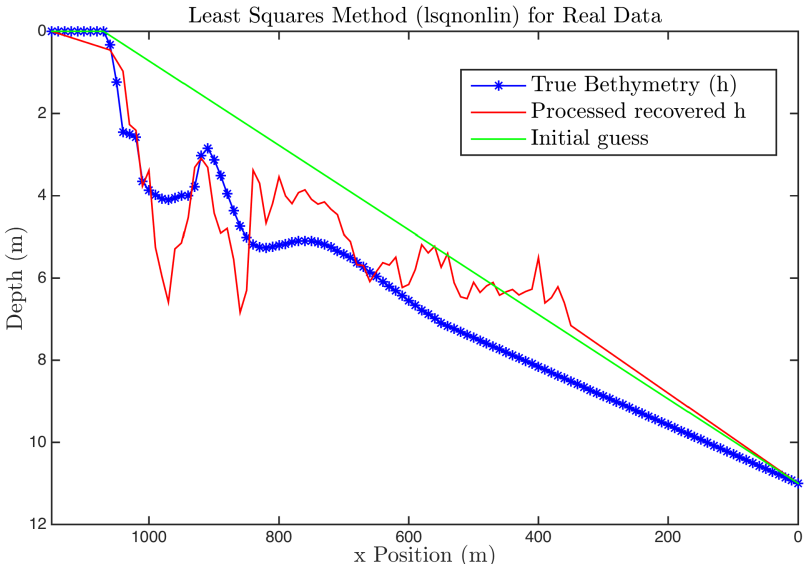

Figure 23: lsqnonlin method reconstruction of depth $\mathbf{h}$ using the simulated data.

5.4 Tikhonov Regularization

$$\hat{\mathbf{h}} = \underset{\mathbf{0} \preceq \mathbf{h} \preceq \mathbf{11}}{\arg\min} \ \|\mathbf{A}(\mathbf{h}) - \mathbf{d}\|_2^2 + \alpha \|\mathbf{h}\|_2^2, \tag{21}$$

[Using the Matlab's fmincon function]

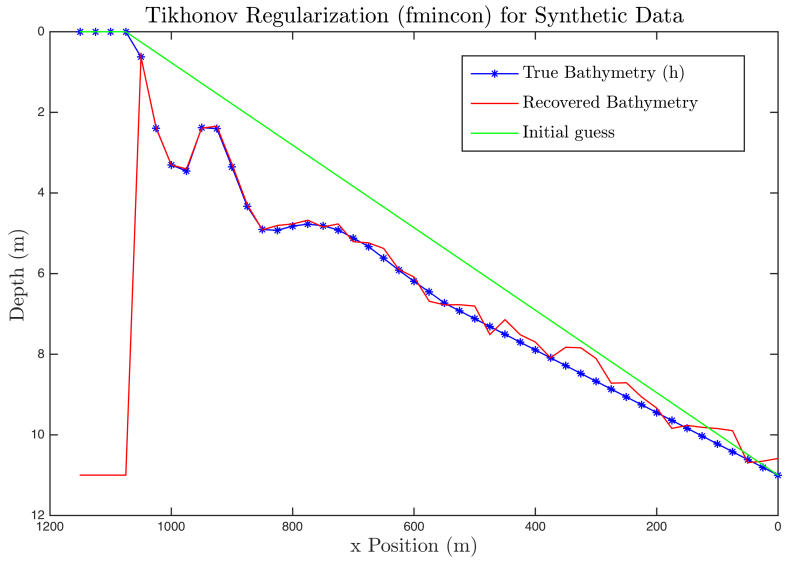

Figure 24: fmincon method reconstruction of depth **h** using the simulated data.

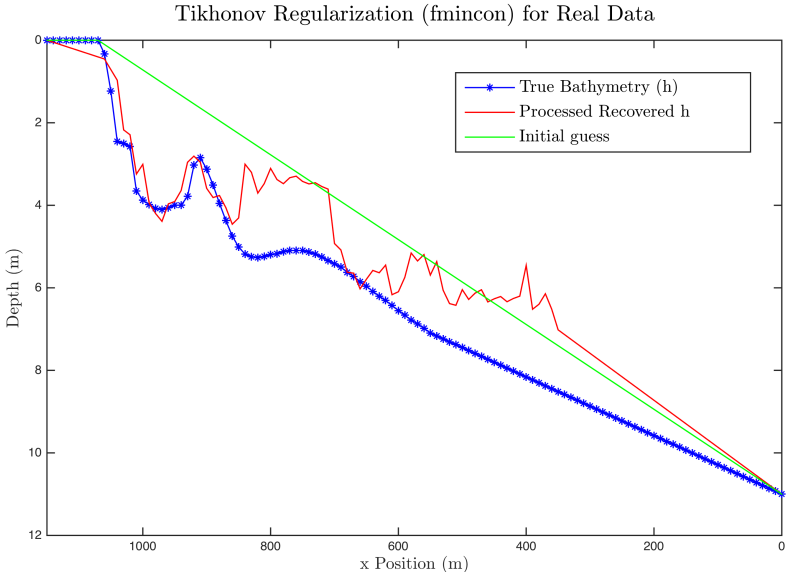

Figure 25: fmincon method reconstruction of depth **h** using the simulated data.

5.5 Bayesian Inference

The Bayesian inversion approach samples a posterior distribution of depth profiles. For comparison to the other inversion methods, we consider only the depth at each grid point which corresponds to the maximum of the posterior probability distribution at that point. This is achieved by taking the maximum of the kernel density of the estimated depth distribution at each point along the 1D profile.

This method is first applied using synthetic k input and the resulting depth estimate is shown in Figure 26. As for other methods, the synthetic result accurately represents the sandbar located at $x \sim 950\ m$ along the profile, which is an important feature to recreate. However, at offshore locations ($x < 600\ m$), the estimation appears to break down. As in other methods, this is expected because of the lower sensitivity of k on h at these depths, a relationship on which our inverse methods rely.

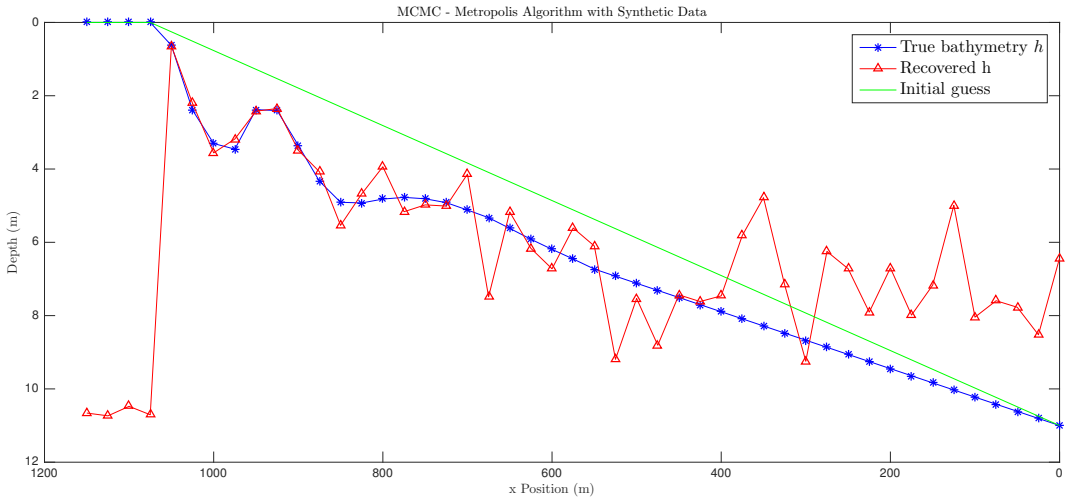

Figure 26: Bathymetry estimate from the Bayesian Markov Chain Monte Carlo approach. The initial h guess is shown in green, the true h is shown in blue, and the derived estimate of h is shown in red.

Real k data is then used to estimate the same bathymetry profile (Figure **??**). We find...

Unlike the other methods, the Bayesian approach results in a distribution of depth profiles which optimize h given uncertain k. Measurements of wave number, k, are not perfect and our resulting distribution of depth profiles translates that uncertainty binto an ensemble of depth estimates which are consistent with the k data to within uncertainty. Figures **??** and **??** show the resulting posterior depth distributions. Note that...

6 Summary and Future Work

Historically, the standard approach for resolving coastal hydrodynamics has been to directly measure bathymetry and use the data as input in numerical models to determine coastal conditions. However, direct measurements of bathymetry are known to be costly in both a temporal and financial sense; requiring heavy project hours and sophisticated equipment. In recent years, remote sensing and photogrammetry have seen rapid advancement, facillitating the easy measurement of surface properties of the coastal environment.

Using three different inversion algorithms, we approximate bathymetry using linear wave theory.

We are using a mathematical approach to estimate bathymetry because waves make it difficult to determine the depth of the ocean physically with technology. Our three methods, nonlinear least squares, Tikhonov regularization, and Bayesian MCMC, prove to have promising results for the estimation of depth given real wave number data.

[Need to solve the following problem with priors $\mathbf{h}_p$].

$$\hat{\mathbf{h}} = \underset{\mathbf{0} \preceq \mathbf{h} \preceq \mathbf{11}}{\arg\min} \ \|\mathbf{A}(\mathbf{h}) - \mathbf{d}\|_2^2 + \alpha \|\mathbf{h} - \mathbf{h}_p\|_2^2, \tag{22}$$

[Want to use proper method to find the optimum regularization parameter α]

- Briefly summarize your contributions, and their possible impact on the field (but don't just repeat the abstract or introduction).
- Identify the limitations of your approach.
- Suggest improvements for future work.
- Outline open problems.

References

[1] Rob Holman, Nathaniel Plant, and Todd Holland. cbathy: A robust algorithm for estimating nearshore bathymetry. *Journal of Geophysical Research: Oceans*, 118(5):2595–2609, 2013.

[2] Nicholas Metropolis, Arianna W Rosenbluth, Marshall N Rosenbluth, Augusta H Teller, and Edward Teller. Equation of state calculations by fast computing machines. *The journal of chemical physics*, 21(6):1087–1092, 1953.

[3] Hilary F Stockdon and Rob A Holman. Estimation of wave phase speed and nearshore bathymetry from video imagery. *Journal of Geophysical Research: Oceans*, 105(C9):22015–22033, 2000.